

A deep learning method for solving high-order nonlinear soliton equation

Shikun Cui^a, Zhen Wang^{a,b,*}, Jiaqi Han^a, Xinyu Cui^a

^a*School of Mathematical Sciences, Dalian University of Technology, Dalian, 116024, China*

^b*Key Laboratory for Computational Mathematics and Data Intelligence of Liaoning Province, Dalian, 116024, China*

Abstract

We propose effective scheme of deep learning method for high-order nonlinear soliton equation and compare the activation function for high-order soliton equation. The neural network approximates the solution of the equation under the conditions of differential operator, initial condition and boundary condition. We apply this method to high-order nonlinear soliton equation, and verify its efficiency by solving the fourth-order Boussinesq equation and the fifth-order Korteweg de Vries equation. The results show that deep learning method can solve the high-order nonlinear soliton equation and reveal the interaction between solitons.

Keywords: deep learning method, physics-informed neural networks, high-order nonlinear soliton equation, interaction between solitons, numerical driven solution.

1. Introduction

Nonlinear soliton equation is an important part of the field of Mathematical Physics, which is used to describe the state or process changing with time in physics, mechanics or other natural sciences[1][2]. As the carrier of soliton theory, the development of nonlinear equation has always been the focus of mathematical physics researchers. In recent years, a deep learning numerical method has been developed to solve many problems related to nonlinear evolution equation. Deep learning method approximate potential solutions by using deep neural network, which is usually more effective than ordinary numerical methods[3][4][5]. Raissi M et al[3] proposed physics-informed neural networks to solve partial differential equation, such neural networks are constrained to respect any symmetries, invariances, or conservation principles. Han et al[6] reconstruct partial differential equations from backward stochastic differential equations, and use neural networks to approximate the gradient of unknown solutions to solve general high-dimensional parabolic partial differential equations. Justin et al[7] used DGM(depth Galerkin method) to study the numerical driven solution of high dimensional partial differential equation. Li and Chen[8][9] used deep learning method to solve many second-order nonlinear evolution equations and many third-order nonlinear evolution equations, such as KdV equation, Burgers equation. They also proposed a new residual neural network to solve the sine-Gordon equation[10]. Wang and Yan[11] study the data-driven solutions of the defocused nonlinear NLS equation by using PINNs. Marcucci G et al[12] studied theoretically artificial neural networks with a nonlinear wave as a reservoir layer and developed a new computing model driven by nonlinear partial differential equations.

At present, deep learning method is only used to solve low-order nonlinear problems or low-order linear problems, and its applicability to high-order nonlinear problems is undiscovered. We apply the deep learning method and physics-informed neural networks[3] to solve high-order nonlinear equation and show the efficiency and effectiveness. Specifically, we will study the numerical driven solutions of the fourth-order Boussinesq equation and the fifth-order KdV equation.

Boussinesq equation, as a kind of nonlinear equation closely related to wave phenomena, has been widely studied in many fields of physics[13][14][15][16][17]. The classical Boussinesq equation describes the evolution of waves in shallow water[13]. Some progress has been made in the analytical solution of Boussinesq equation[18][19][20][21].

KdV equation has always been an important part of nonlinear mathematical and physical model, and it is also a hotspot of numerical methods[25][26][27]. The numerical solution of the fifth-order KdV equation has also made some progress[28][29][30]. The numerical driven solution of KdV equation has been solved by Raissi M et al[3]

*School of Mathematical Sciences, Dalian University of Technology, Dalian, 116024, China

Email address: wangzhen@dlut.edu.cn (Zhen Wang)

and Li, Chen[9], Raissi M et al used discrete time model to solve KdV equation, Li and Chen used continuous time model to solve KdV equation. However, due to the complexity of high-order nonlinear equation, the numerical driven solution of high-order nonlinear problem have not been solved. We will illustrate the applicability of the deep learning method to the fifth-order nonlinear soliton equation by solving the fifth-order KdV equation.

The paper is organized as follows. In section 2, we will introduce the method of deep learning to solve high-order equations. In section 3, we use the deep learning method to reproduce the one-soliton and the two-soliton numerical driven solution of the fourth-order Boussinesq equation. In numerical driven solution, we find the dynamic behavior of solitons interaction. Specifically, we solve the chasing-soliton and colliding-soliton of Boussinesq equation, and find the dynamic behavior between solitons from the numerical driven solution. In section 4, we get the one-soliton numerical driven solution and the two-soliton numerical driven solution of the fifth-order KdV equation. In the numerical driven solution, we also find the dynamic behavior of solitons interaction. Finally, some concluding discussions and remarks are contained in section 5.

2. Method

We consider the following form of $(1 + 1)$ -dimensional fourth-order and fifth-order nonlinear soliton equation,

$$\chi_1(u_t, u_{tt}) = \chi_2(u, u_x, u_{xx}, u_{xxx}, u_{xxxx}, u_{xxxxx}), \quad (1)$$

and solve their soliton solution, where the subscripts t and x denote the partial derivatives, and χ_1 is a linear function of the time derivative of $u(x, t)$, χ_2 is a nonlinear function of $u(x, t)$ and its partial derivative to space variable x . Specifically, we build a multi-layer neural network to approximate the potential solution, and use the automatic differentiation technique to obtain its derivatives in time and space[31].

The residual network is defined

$$f = \chi_1(u_t, u_{tt}) - \chi_2(u, u_x, u_{xx}, u_{xxx}, u_{xxxx}, u_{xxxxx}). \quad (2)$$

The shared parameters of neural networks can be learned by minimizing the loss of mean square error,

$$LOSS = LOSS_u + LOSS_f, \quad (3)$$

$$LOSS_u = \frac{1}{N_u} \sum_{n=1}^{N_u} |u(t_u^i, x_u^i) - u^i|, \quad (4)$$

$$LOSS_f = \frac{1}{N_f} \sum_{n=1}^{N_f} |f(t_f^i, x_f^i)|.$$

$LOSS_u$ is the mean square error of initial and boundary, $LOSS_f$ is the internal calculation error, t_u^i and x_u^i represent the initial and boundary training values, t_f^i and x_f^i are the point collected in f . N_u is the total number of selected boundary points and initial points, N_f is the total number of selected internal collection points. A common deep feedforward neural fully connected network used to deal with high-order nonlinear problems. Figure 1 shows the framework of physics-informed neural networks. There are activation function, weights and bias between each layer. PINNs updates weights and biases by reducing error $LOSS$, and the neural network stops operation until the error is lower than the specified standard.

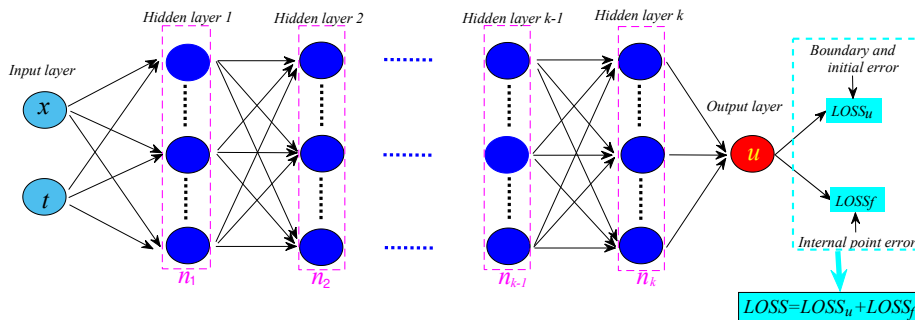


Figure 1: Architecture of physics-informed neural networks

Where k represent the number of hidden layers, n_k represents the number of neurons corresponding to the hidden layer. We will improve the neural network from the following aspects to ensure that PINNs can deal with high-order nonlinear problems. Firstly, we will determine the appropriate number of hidden layers and the corresponding number of neurons. Secondly, we will improve the efficiency of neural network by improving the activation function.

In high-order nonlinear problem, it is very important to select the number of hidden layers and neurons in each layer. If the selected neural network structure is not suitable, there will occur over fitting(the deep learning model is superior in training set, but the final result is not good), under fitting(the deep learning model does not capture the characteristics of the data well and can not solve the equation well), loss of operational efficiency and other problems easily. Compared with low-order problems, high-order nonlinear problems are more difficult due to the complexity of their equation. Through a large number of experiments, we decide to use a neural network with four hidden layers to deal with high-order nonlinear soliton equation.

On the selection of activation function, Chen and Li[9] proved that trigonometric function as activation function is effective on solitary wave solution of third-order nonlinear soliton equation. In this paper, we will study the deep learning algorithm of high-order nonlinear soliton equation and explore the effectiveness of trigonometric function as activation function for high-order nonlinear soliton equation and find the most suitable activation function. In addition, we use L-BFGS optimization algorithm[31] to set all parameters of the target to minimize the loss function Equation (3). All numerical examples reported here are run on a Dell computer with Intel Xeon Gold 6320R i5 processor and 32 GB memory.

3. Boussinesq equation

Boussinesq equation with Dirichlet boundary condition and initial condition given by

$$\begin{cases} u_{tt} - u_{xx} - u_{xxxx} - 3(u^2)_{xx} = 0, x \in [-20, 20], t \in [-5, 5], \\ u(x, -5) = u_0(x), \\ u(-20, t) = u(20, t), \end{cases} \quad (5)$$

where $u_0(x)$ is a given real valued smooth function.

We use the deep learning method to find the one-soliton and two-soliton numerical driven solution of equation (5) with tanh as activation function, and try to reproduce the dynamic behavior between solitons.

3.1. One-soliton solution

In this subsection, the numerical driven one-soliton solution of Boussinesq equation will be solved. The one-soliton analytic solution of Boussinesq equation can be obtained by using Hirota method[18][19],

$$u(x, t) = \frac{k_1^2}{2} \operatorname{sech}^2 \left(\frac{k_1 x + \sqrt{k_1^2 + k_1^4} t}{2} + \xi_0 \right). \quad (6)$$

We could set $k_1 = 1, \xi_0 = 0$. The corresponding initial condition becomes

$$u_0(x) = \frac{1}{2} \operatorname{sech}^2 \left(\frac{x - 5\sqrt{2}}{2} \right). \quad (7)$$

We generate the data of 201 snapshots directly on regular space-time grid with $\Delta t = 0.05s$. A small training data subset is generated by randomly latin hypercube sampling method[24], the number of collection points are $N_u = 100, N_f = 20000$. The latent solution $u(t, x)$ can be learned by minimizing the loss function Equation (3). Top panel of Figure 2 shows comparison of the predicted spatiotemporal solution and exact solution. The model achieves a relative L^2 error of size 2.0×10^{-2} in a runtime of 152s. The model is iterated 170 times to complete the operation. Bottom panel of Figure 2 shows the detailed comparison of exact solution and predicted spatiotemporal solution at different times $t = -2.5, t = 0, t = 2.5$ respectively. One-soliton solution of Boussinesq equation is reconstructed by using deep learning method accurately. From Figure 3, we can clearly observe the reconstructed solitary wave motion.

In order to verify the universality of our neural network architecture for the one-soliton solution of Boussinesq equation, we try to change the value of k_1 and give the numerical solution respectively. The results shows that our neural network architecture is effective in solving one-soliton of Boussinesq equation.

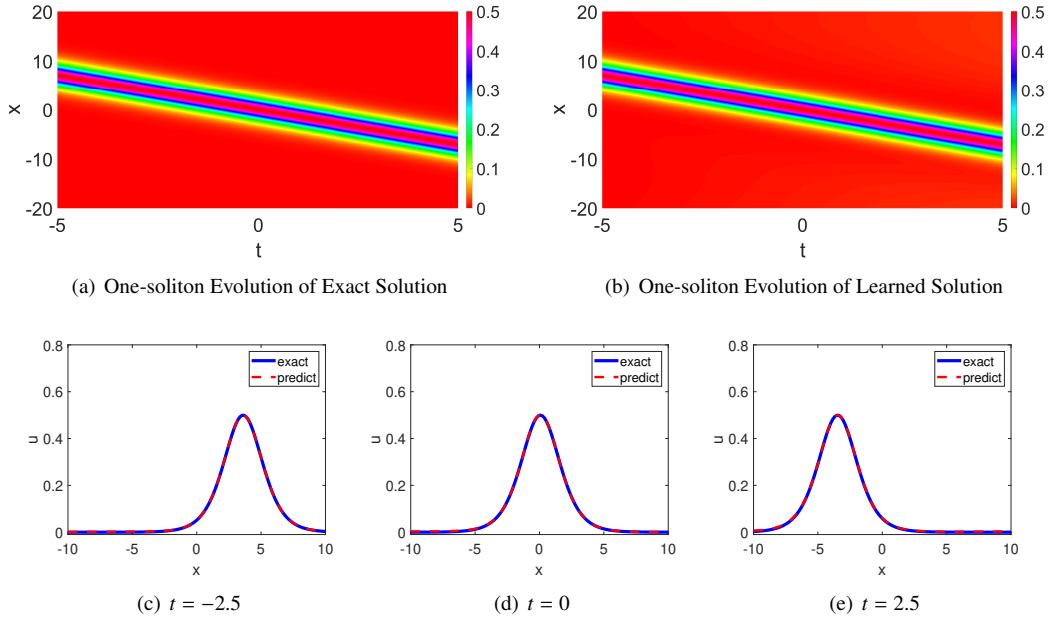


Figure 2: Subgraph (a) and (b) are comparison of one-soliton exact solution and learned solution of Boussinesq equation, subgraph (c)-(e) are the detailed comparison of exact solution and learned spatiotemporal solution at the specific time.

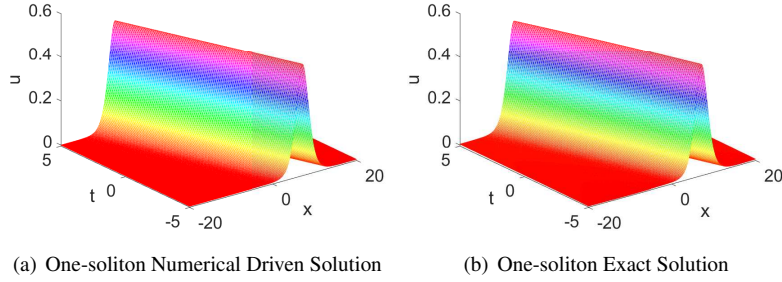


Figure 3: Spatiotemporal evolution of one-soliton numerical driven solution and exact solution of Boussinesq equation.

Table 1: The results of different one-soliton solution of Boussinesq equation calculated by deep learning method.

k_1	0.8	0.9	1.0	1.1	1.2	1.3	1.4
L^2 error	2.79×10^{-2}	3.36×10^{-2}	2.03×10^{-2}	1.9×10^{-2}	1.67×10^{-2}	1.60×10^{-2}	1.62×10^{-2}
Time(s)	224	191	152	160	294	284	480
Iterations	141	155	170	195	576	416	753

3.2. Two-soliton solution

In this subsection, we will calculate the numerical driven two-soliton solution of the Boussinesq equation and reproduce the solitons interaction process. The two-soliton solution of Boussinesq equation is given[18][19].

$$\begin{aligned}
 u(x, t) = & 2 \frac{k_1^2 e^{k_1 x + \omega_1 t + \delta_1} + k_2^2 e^{k_2 x + \omega_2 t + \delta_2} + (k_1 + k_2)^2 e^{(k_1 + k_2)x + (\omega_1 + \omega_2)t + \delta_1 + \delta_2 + \delta_0}}{1 + e^{k_1 x + \omega_1 t + \delta_1} + e^{k_2 x + \omega_2 t + \delta_2} + e^{(k_1 + k_2)x + (\omega_1 + \omega_2)t + \delta_1 + \delta_2 + \delta_0}} \\
 & - 2 \frac{(k_1 e^{k_1 x + \omega_1 t + \delta_1} + k_2 e^{k_2 x + \omega_2 t + \delta_2} + (k_1 + k_2) e^{(k_1 + k_2)x + (\omega_1 + \omega_2)t + \delta_1 + \delta_2 + \delta_0})^2}{(1 + e^{k_1 x + \omega_1 t + \delta_1} + e^{k_2 x + \omega_2 t + \delta_2} + e^{(k_1 + k_2)x + (\omega_1 + \omega_2)t + \delta_1 + \delta_2 + \delta_0})^2}, \\
 e^{\delta_0} = & - \frac{(\omega_1 - \omega_2)^2 - (k_1 - k_2)^2 - (k_1 - k_2)^4}{(\omega_1 + \omega_2)^2 - (k_1 + k_2)^2 - (k_1 + k_2)^4},
 \end{aligned} \tag{8}$$

where δ_1 and δ_2 is constant, ω_1 and ω_2 meet the conditions $\omega_1^2 = k_1^2 + k_1^4$, $\omega_2^2 = k_2^2 + k_2^4$ respectively.

Two-soliton solution of Boussinesq equation have two states, colliding-soliton(the two solitons have different

directions) and chasing-soliton(the two solitons have the same direction and different amplitude). We will find the numerical driven solution of the two forms respectively, and study their dynamic behavior and the interaction between solitons.

3.2.1. Colliding-soliton

We just set $k_1 = k_2 = 1.1$, $\delta_1 = \delta_2 = 0$, ω_1 and ω_2 have opposite sign. We generate the data of 201 snapshots directly on regular space-time grid with $\Delta t = 0.05s$. A small training data subset is generated by randomly latin hypercube sampling method[24], the number of collection points are $N_u = 100$, $N_f = 25000$. The latent solution $u(x, t)$ is learned by minimizing the loss function Equation (3). Top panel of Figure 4 shows the comparison of predicted spatiotemporal solution and exact solution. Bottom panel of Figure 4 shows the detailed comparison of actual solution and predicted spatiotemporal solution at different time $t = -4.5$, $t = 0$, $t = 2.5$ respectively. The specific spatiotemporal evolution of colliding-soliton of Boussinesq equation is given in Figure 5. The model achieves a relative L^2 error of size 7.63×10^{-2} in a runtime of 430s. The model is iterated 578 times to complete the operation.

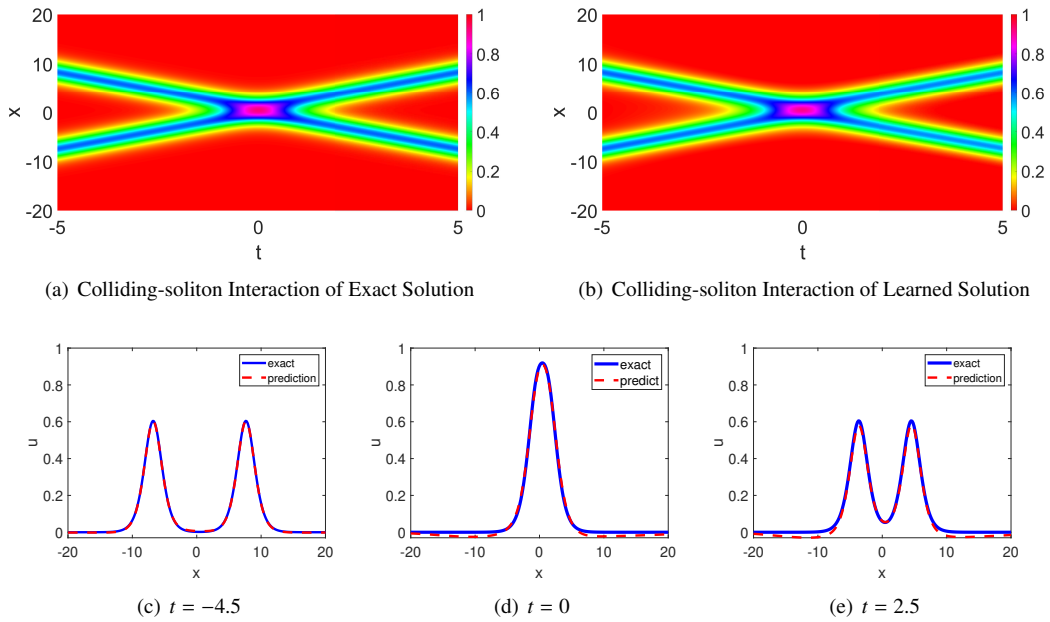


Figure 4: Subgraph (a) and (b) are comparison of colliding-soliton exact solution and learned solution of Boussinesq equation, subgraph (c)-(e) are the detailed comparison of exact solution and learned spatiotemporal solution at the specific time.

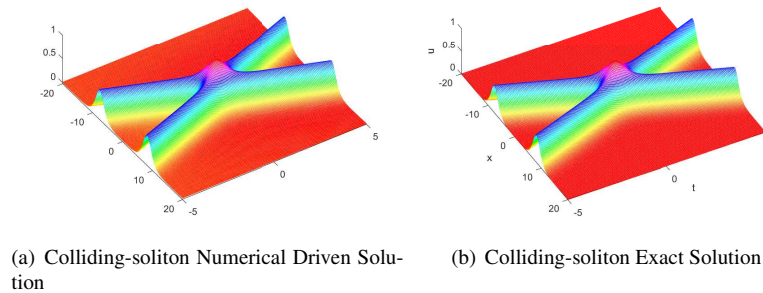


Figure 5: Spatiotemporal evolution of colliding-soliton numerical driven solution and exact solution.

From Figure 5, we learn the spatiotemporal evolution process of separation-fusion-separation of colliding-soliton. Amplitude becomes high during the colliding process and shape remains unchanged before and after the interaction, which is consistent with the known fact. The ‘phase shift’ phenomenon also occur in numerical driven solution.

In order to verify the universality of our neural network architecture for the colliding-soliton, we calculate the different colliding-soliton solutions of Boussinesq equation by deep learning method. The result shows that the deep learning method is effective in solving the colliding-soliton solution of Boussinesq equation.

Table 2: The results of different colliding-soliton solution of Boussinesq equation calculated by deep learning method.

k_1	0.8	0.9	1.0	1.1	1.2
k_2	0.8	0.9	1.0	1.1	1.2
L^2 error	8.55×10^{-2}	8.10×10^{-2}	1.16×10^{-1}	7.63×10^{-2}	7.64×10^{-2}
time(s)	358	551	642	430	1065
Iterations	320	635	801	578	755

3.2.2. Chasing-soliton

We could set $k_1 = 1.5$, $k_2 = 0.9$, $\delta_1 = \delta_2 = 0$, ω_1 and ω_2 are positive. In this condition, two-solitons have same direction and different magnitude, so the soliton chasing phenomenon occurs. We generate the data of 201 snapshots directly on the regular space-time grid with $\Delta t = 0.05s$. A small training data subset is generated by randomly latin hypercube sampling method[24], the number of collection points are $N_u = 100$, $N_f = 25000$. Top panel of 6 shows the comparison of predicted spatiotemporal solution and exact solution. Bottom panel of Figure 6 shows the detailed comparison of exact solution and learned spatiotemporal solution at different time $t = -4.5$, $t = 0$, $t = 2.5$ respectively. The model achieves a relative L^2 error of size 6.73×10^{-2} in a runtime of 892s.

Figure 7 shows the spatiotemporal evolution process of separation-fusion-separation. Amplitude becomes low during the fusion process and shape remains unchanged before and after the interaction, which is consistent with the known fact. We also observe the ‘phase shift’ phenomenon in the chasing-soliton numerical driven solution.

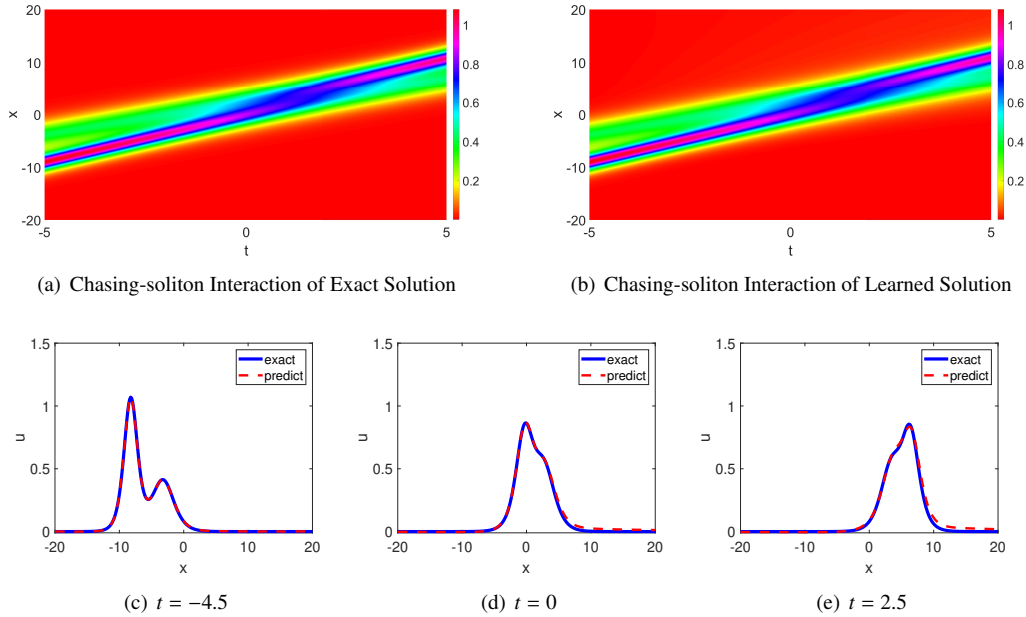


Figure 6: Subgraph (a) and (b) are comparison of chasing-soliton exact solution and learned solution of Boussnesq equation, subgraph (c)-(e) are the detailed comparison of exact solution and learned spatiotemporal solution at the specific time.

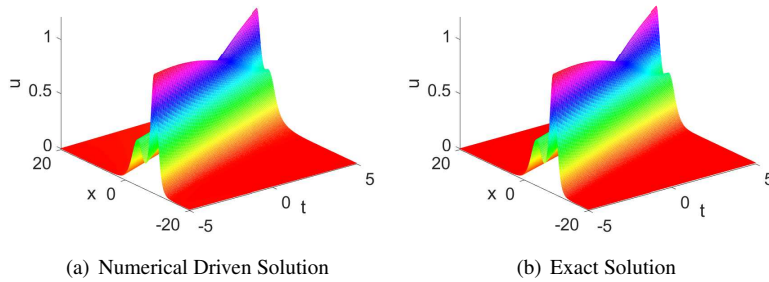


Figure 7: Spatiotemporal evolution of chasing-soliton numerical driven solution and exact solution.

In exploring the effectiveness of activation function, we find tanh function is more effective than trigonometric function. We take one-soliton solution as an example, the calculation results is shown in Tabel 3. We find that both tanh and trigonometric function is useful in Boussinesq equation, and tanh cost less computational source. Compared with one-soliton solution, the two-soliton solution of Boussinesq equation cost more computational source.

Table 3: The results of different activation function of one-soliton calculated by deep learning method.

activation function	tanh	cos	sin	sigmoid	relu
L^2 error	1.97×10^{-2}	1.86×10^{-1}	1.27×10^{-1}	9.22×10^{-1}	8.37×10^{-1}
time(s)	160	1670	1531	105	16
Iterations	195	4722	3080	0	4

4. Fifth-order KdV equation

In this section, we consider the fifth-order KdV equation with Dirichlet periodicity boundary condition and initial condition,

$$\begin{cases} u_t + (\alpha u_{xxxx} + \beta u u_{xx} + \gamma u^3)_x = 0, x \in [-10, 10], t \in [0, 2\pi], \\ u(x, 0) = u_0(x), \\ u(-10, t) = u(10, t), \end{cases} \quad (9)$$

where α, β, γ are arbitrary constant, $u_0(x)$ is a given real valued smooth function.

We choose cos as activation function, and explore the effectiveness of trigonometric function as activation function of the fifth-order KdV equation. A deep learning method is used to find the one-soliton and two-soliton solution of the equation, and reproduce the dynamic behavior between the solitons.

4.1. One-soliton solution

Using Hirota bilinear method, the one-soliton analytical solution of fifth-order KdV equation (9) can be obtained[23],

$$u(x, t) = \frac{15\alpha k_1^2}{2\beta} \operatorname{sech}^2\left(\frac{k_1 x - \alpha k_1^5 t + \xi_0}{2}\right). \quad (10)$$

We set $\alpha=1, \beta=15, \gamma=15, k_1 = 1, \xi_0 = 3$, the equation is also called C-D-J-K equation. Correspondingly,

$$u_0(x) = \frac{1}{2} \operatorname{sech}^2\left(\frac{x}{2} - 1\right). \quad (11)$$

In order to obtain high-precision data set, we generate the data of 201 snapshots directly on the regular space-time grid with $\Delta t = 0.05s$. A small training data subset is generated by randomly latin hypercube sampling method [24], the number of collection points are $N_u = 100, N_f = 20000$. Top panel of Figure 8 shows the comparison of predicted spatiotemporal solution and exact solution, and bottom panel of Figure 8 shows the detailed comparison of exact solution and predicted spatiotemporal solution at different time $t=1.57, t=3.14, 4.71$ respectively. Figure 9 shows specific spatiotemporal evolution of one-soliton solution of fifth-order KdV equation. The model achieves a relative L^2 error of size 1.36×10^{-2} in a runtime of 537s. The model is iterated 803 times to complete the operation.

From Figure 8 and Figure 9, we learn that velocity and shape of the numerical driven solution of the one-soliton remain unchanged during the motion, which shows the dynamic behavior of the soliton well.

To verify the universality of our neural network architecture for the one-soliton numerical driven solution of fifth-order KdV equation, we calculate the different one-soliton solution of fifth-order KdV equation. The result shows that the our neural network architecture is very effective in solving one-soliton solution of fifth-order KdV equation.

Table 4: The results of different one-soliton solution of fifth-order KdV equation calculated by deep learning method.

k_1	0.9	0.95	1.0	1.05	1.1
L^2 error	1.47×10^{-2}	2.57×10^{-2}	1.36×10^{-2}	4.64×10^{-2}	2.36×10^{-2}
time(s)	687	680	537	600	1166
Iterations	300	803	803	883	1604

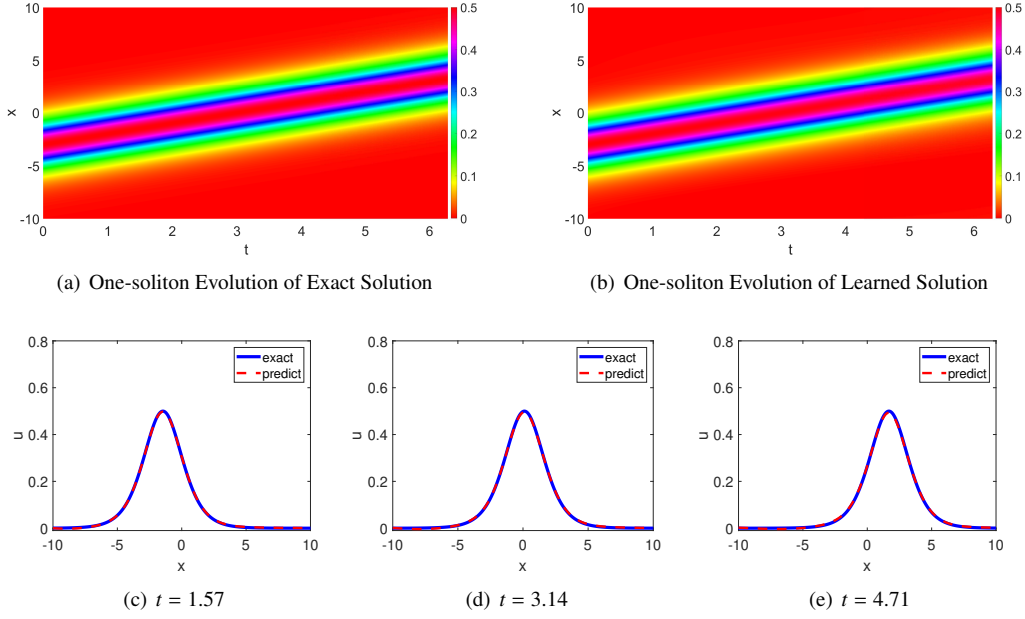


Figure 8: Subgraph (a) and (b) are comparison of one-soliton exact solution and learned solution of fifth-order KdV equation, subgraph (c)-(e) are the detailed comparison of exact solution and learned spatiotemporal solution at the specific time.

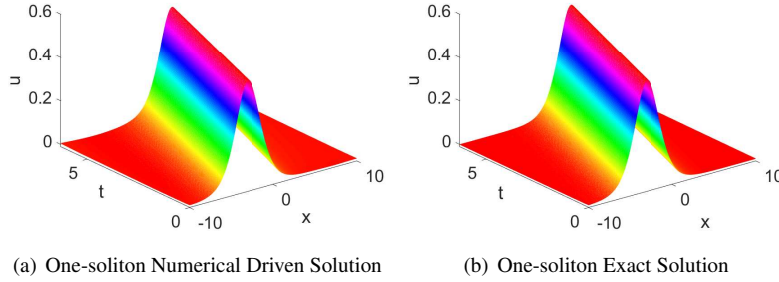


Figure 9: Spatiotemporal evolution of one-soliton numerical driven solution and exact solution of fifth-order KdV equation

4.2. Two-soliton solution

In order to observe the solitons interaction behavior well, we set $x \in [-20, 20]$ and $t \in [-5, 5]$. Equation (9) becomes

$$\begin{cases} u_t + (u_{xxxx} + 15uu_{xx} + 15u^3)_x = 0, & x \in [-20, 20], t \in [-5, 5], \\ u(x, 0) = u_0(x), \\ u(-20, t) = u(20, t). \end{cases} \quad (12)$$

By using Hirota bilinear method, the two-soliton analytical solution of fifth-order KdV Equation (12) can be obtained[23]

$$u(x, t) = 2 \frac{k_1^2 e^{k_1 x + \omega_1 t + \delta_1} + k_2^2 e^{k_2 x + \omega_2 t + \delta_2} + (k_1 + k_2)^2 e^{(k_1 + k_2)x + (\omega_1 + \omega_2)t + \delta_1 + \delta_2 + \delta_0}}{1 + e^{k_1 x + \omega_1 t + \delta_1} + e^{k_2 x + \omega_2 t + \delta_2} + e^{(k_1 + k_2)x + (\omega_1 + \omega_2)t + \delta_1 + \delta_2 + \delta_0}} - 2 \frac{(k_1 e^{k_1 x + \omega_1 t + \delta_1} + k_2 e^{k_2 x + \omega_2 t + \delta_2} + (k_1 + k_2) e^{(k_1 + k_2)x + (\omega_1 + \omega_2)t + \delta_1 + \delta_2 + \delta_0})^2}{(1 + e^{k_1 x + \omega_1 t + \delta_1} + e^{k_2 x + \omega_2 t + \delta_2} + e^{(k_1 + k_2)x + (\omega_1 + \omega_2)t + \delta_1 + \delta_2 + \delta_0})^2}, \quad (13)$$

$$\omega_1 = -k_1^5, \omega_2 = -k_2^5, e^{\delta_0} = \frac{(k_1 - k_2)^2 + (k_1^2 - k_1 k_2 + k_2^2)}{(k_1 + k_2)^2 + (k_1^2 + k_1 k_2 + k_2^2)}.$$

We could set $k_1 = 1, k_2 = 0.8, \xi_1 = \xi_2 = 0$. In order to obtain high-precision data set, we generate the data of 201 snapshots directly on the regular space-time grid with $\Delta t = 0.05s$. A small training data subset is generated by randomly latin hypercube sampling [24], the number of collection points are $N_u = 100, N_f = 20000$. Top panel of Figure 10 shows the comparison of predicted spatiotemporal solution and exact solution. Bottom panel of Figure

10 shows the detailed comparison of exact solution and predicted spatiotemporal solution at different time $t = -4.5, t = 0, t = 2.5$ respectively. Specific spatiotemporal evolution of two-soliton is given in Figure 11. The model achieves a relative L^2 error of size 7.22×10^{-2} in a runtime of 1774s. The model is iterated 3606 times to complete the operation.

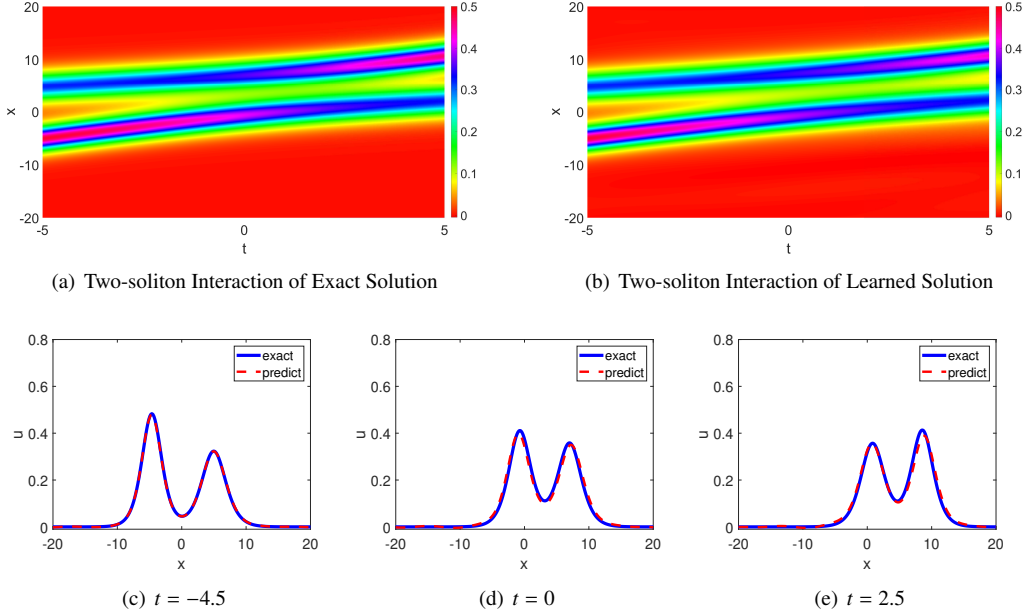


Figure 10: Subgraph (a) and (b) are comparison of two-soliton exact solution and learned solution of fifth-order KdV equation, subgraph (c)-(e) are the detailed comparison of exact solution and learned spatiotemporal solution at the specific time.

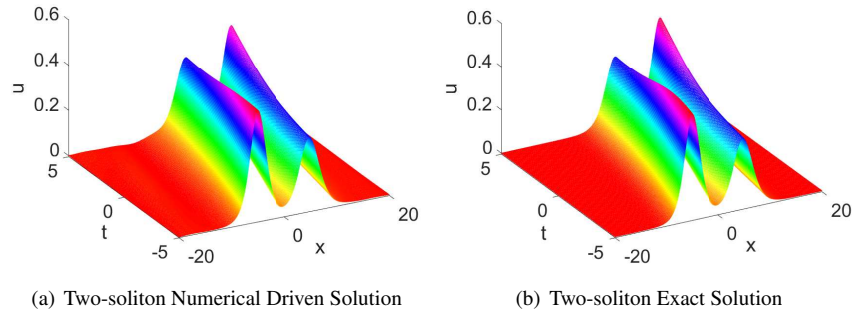


Figure 11: Spatiotemporal evolution of two-soliton numerical driven solution and exact solution of fifth-order KdV equation

On the selection of activation function, we try a lot of other activation functions of two-soliton, the results is given in Figure 5. The result shows that the trigonometric function is more effective in solving the fifth-order KdV equation.

Table 5: The results of different activation function of two-soliton calculated by deep learning method.

activation function	tanh	cos	sin	sigmoid	relu
L^2 error	1.46×10^{-1}	7.22×10^{-2}	1.27×10^{-1}	8.18×10^{-1}	6.13×10^{-1}
time(s)	623	1740	1531	237	48
Iterations	1390	3600	3080	0	5

In addition, a small amplitude noise is given to verify the rationality of the structure of the fifth-order KdV equation neural network. The results show that the deep learning method is effective in solving two-soliton solutions of fifth-order KdV equation.

Table 6: The results of different two-soliton solution of fifth-order KdV equation calculated by deep learning method.

k_1	1.0	0.99	1.01	1.0	1.0
k_2	0.8	0.8	0.8	0.79	0.81
L^2 error	7.22×10^{-2}	8.27×10^{-2}	1.05×10^{-1}	9.05×10^{-2}	1.0×10^{-1}
time(s)	1774	913	1011	1000	657
Iterations	3606	1654	1738	2224	1240

5. Summary and discussion

We find a neural network architecture of PINNs suitable for solving high-order nonlinear soliton equation. Specifically, it has four hidden layers, the number of corresponding neurons are 256, 128, 64, 32 and 40, 40, 40, 40. And we study the numerical driven solution of high-order nonlinear problems (fourth-order Boussinesq equation and fifth-order KdV equation), and control L^2 error to 10^{-2} magnitude, which shows that the deep learning method is effective. We extend the deep learning method to the solution of fourth-order and fifth-order equation, but the ability of deep learning method to deal with higher-order equation still needs to be explored. We summarize the conclusions as follows. Firstly, the deep learning method is suitable to solve the soliton solution of fourth-order Boussinesq equation and fifth-order KdV equation. The deep learning method can recover the dynamic behavior of solitons in high-order nonlinear soliton equation. From numerical driven solution, we can observe the ‘phase shift’ phenomenon, and the shape remains unchanged after the interaction, which is consistent with known facts. Secondly, trigonometric function is effective in high-order nonlinear problems. Compared with the low-order problem, high-order problems have higher sensitivity in selection of architecture of neural network.

Acknowledgment

Project supported by LiaoNing Revitalization Talents Program (XLYC1907014) and “the Fundamental Research Funds for the Central Universities” (DUT21ZD205).

Reference

References

- [1] Mayers J 2008 Phys. Rev. A 78 3 033618
- [2] Manojlovic N and Marugan GAM 1995 Int. J. Mod. Phys. D 4 6 749-766
- [3] Raissi M, Perdikaris P and Karniadakis G E 2017 J. Comput.Phys. 348 686-707
- [4] Lagaris I E, Likas A and Fotiadis D I 1998 IEEE Trans. Neural Networks 9 987-1000
- [5] Raissi M and Karniadakis G E 2018 J. Comput. Phys. 357 125-141
- [6] Han J, Jentzen A and Weinan E 2018 Proc. Natl. Acad. Sci. 115 8505-8510
- [7] Sirignano J and Spiliopoulos K 2018 J.Comput.Phys. 375 1339-1364
- [8] Li J and Chen Y 2020 Commun. Theor. Phys. 72 105005
- [9] Li J and Chen Y 2020 Commun. Theor. Phys. 72 115003
- [10] Li J and Chen Y 2021 Commun. Theor. Phys. 73 015001
- [11] Wang L and Yan ZY 2021 Phys. Lett. A 404 127408
- [12] Marcucci G, Pierangeli D and Conti C 2020 Phys. Rev. Lett. 125 9 093901
- [13] Boussinesq J 1872 J. Math. Pures Appl. 17 55-108
- [14] Ursell F 1953 Proc. Cambridge Philos. Soc. 49 4 685-694
- [15] Lu CN, Fu C and Yang HW 2018 Appl. Math. Comput. 327 104-116
- [16] Guo BX, Gao ZJ and Lin J 2016 Commun. Theor. Phys. 66 6 589-594
- [17] Himonas AA and Mantzavinos D 2015 J. Differ. Equ. 134 1 62-100
- [18] Zhang Y, Ye LY, Lv YN and Zhao HQ 2007 J. Phys. A-Math. Theor. 40 21 5539-5549
- [19] Hietarinta J 1987 J. Math. Phys. 28 8 1732-1742
- [20] Zhang L, Zhang LF and Li CY 2008 Chin. Phys. B 17 2 403-410
- [21] Clarkson PA 2008 Anal. Appl. 6 4 349-369
- [22] Moleleki LD 2014 Adv. Math. Phys. 2014 672679
- [23] Hietarinta J 1987 J. Math. Phys. 28 9 2094-2101
- [24] Stein M L 1987 Technometrics 29 143-151
- [25] Kuo PY and Wu HM 1981 J. Math. Anal. Appl. 82 2 334-345
- [26] Vliegenthart Ac 1971 J. Eng. Math. 5 2 137-155
- [27] Zhang YN, Tam HW and Hu XB 2014 J. Phys. A-Math. Theor. 47 4 045202
- [28] Hu WP and Deng ZC 2008 Chin. Phys. B 17 11 3923-3929
- [29] Ahmad H, Khan TA and Yao SW 2020 Open Math. 18 738-748
- [30] Kaya D 2003 Appl. Math. Comput. 144 2-3 353-363
- [31] Liu D C and Nocedal J 1989 Math. Program. 45 503-528